

Cite this: *RSC Sustainability*, 2023, 1, 1177Received 20th March 2023  
Accepted 3rd July 2023

DOI: 10.1039/d3su00095h

rsc.li/rscsus

# Charting a path to catalytic upcycling of plastic micro/nano fiber pollution from textiles to produce carbon nanomaterials and turquoise hydrogen†

Silvia Parrilla-Lahoz,<sup>a</sup> Marielis C. Zambrano,<sup>b</sup> Vlad Stolojan,<sup>id</sup><sup>a</sup> Rachida Bance-Soualhi,<sup>a</sup> Joel J. Pawlak,<sup>b</sup> Richard A. Venditti,<sup>ib</sup><sup>b</sup> Tomas Ramirez Reina<sup>ib</sup><sup>ac</sup> and Melis S. Duyar<sup>id</sup><sup>\*a</sup>

Washing synthetic textile fibers releases micro/nano plastics, endangering the environment. As new filters and associated regulations are developed to prevent fiber release from washing machines, there emerges a need to manage the collected waste, for which the only current options are combustion or landfill. Herein we show for the first time the application of a catalytic pyrolysis approach to upcycle textile derived fibrous micro/nano plastics waste, with the aim of keeping carbon in the solid phase and preventing its release as a greenhouse gas. Herein, we demonstrate the co-production of hydrogen and carbon nanomaterials from the two most prevalent global textile microfiber wastes: cotton and polyester. Our results pave a way forward to a realistic process design for upcycling mixed micro/nano fiber waste collected from laundering, drying, vacuuming, and environmental cleanup.

## Sustainability spotlight

Microplastics have already contaminated the entire planet. The situation is made worse by washing synthetic clothes, as micro/nano sized plastics are released from textile fibres. While there are emerging initiatives to fit washing machines with filters to collect plastic microfibrils, once collected, the fibres will either be landfilled or combusted due to a lack of alternative solutions. These disposal methods mean that while addressing UN Sustainable Development goal 14 of protecting life below water, the current methods unfortunately move the problem of microplastics to landfills (jeopardising UN SDG 15) and create additional risk to our climate upon combustion (UN SDG 13). Herein we take an upcycling approach to manage microfibre waste, while keeping the carbon contained within as a solid product and preventing release of greenhouse gases, in alignment with UN SDGs 13, 14 and 15.

## Introduction

From 2 million metric tonnes in 1950 to 390.7 million in 2021, plastic manufacturing has grown dramatically (4%) and is predicted to double within 20 years.<sup>1,2</sup> China is the world's largest producer of plastics, accounting for 32% of global production in 2021.<sup>2</sup> Weathering and aging turn most discarded and mismanaged plastics into micro/nano plastics. Micro/nano plastics have gained increased attention in recent years as they are present in land, air, and water in alarmingly large quantities.<sup>3</sup> Due to their small size and large surface-to-volume ratio, micro/nano plastics can also sorb and accumulate pollutants which they can then transfer to organisms, causing toxicity

across the food chain. In addition to this, the additives present in plastics (plasticizers, UV blockers, *etc.*) can also release toxins and interact with adjacent pollutants.<sup>3</sup>

Synthetic textiles contribute heavily to microplastics release, making up 35% of primary microplastics released to the environment.<sup>4</sup> The natural textile cotton and the synthetic textile polyester (PET) make up most of the fabrics used in clothing. While alternative methods like the Lyocell spinning process can also be used for recycling cotton waste,<sup>5,6</sup> it is essential to evaluate the suitability and feasibility of the produced microfibers for large-scale production of Lyocell in terms of yield and purity. Moreover, the presence of polyester contamination presents additional obstacles in extracting cellulose for fiber spinning processes. In this context, pyrolysis emerges as a more robust approach capable of effectively handling anticipated contaminants and facilitating the utilization of cotton, polyester, and other materials. It should be noted that recycling and pyrolysis techniques are not mutually exclusive, as textiles cannot be recycled indefinitely. Micro/nanofibers from garment finishing, laundering, drying, and even wearing are often mixed synthetic and natural fibers, with no central collection or processing mechanism, making pollution abatement difficult. However, it is important to clarify that some studies showed

<sup>a</sup>School of Chemistry and Chemical Engineering, University of Surrey, Guildford, GU2 7XH, UK. E-mail: m.duyar@surrey.ac.uk

<sup>b</sup>Department of Forest Biomaterials, College of Natural Resources, North Carolina State University, Raleigh, North Carolina 27695-8005, USA

<sup>c</sup>Inorganic Chemistry Department & Material Science Institute, University of Seville-CSIC, Avda. Américo Vespucio 49, Sevilla, 41092, Spain

† Electronic supplementary information (ESI) available. See DOI: <https://doi.org/10.1039/d3su00095h>



polyester (synthetic) garments to remain largely intact after 200 days in seawater, but natural fibers such as cotton and cellulose fabrics were shown to degrade after 30 days.<sup>7–9</sup> In terms of environmental damage, the present research indicates that the two types of fibers do not behave the same. However, because it is not possible to separate collected micro/nanofibers, it is crucial to understand the behaviour of both types of fibers under the same thermochemical upcycling technique, to utilise thermochemical conversion as a means to process a thoroughly mixed feedstock of natural and synthetic fibres. While reduction and substitution of plastics use are necessary to prevent pollution, there are also significant efforts underway to capture the generated waste, such as by fitting washing machines with filters. California, France, and Australia are already fighting microfibre pollution. After January 2029, all residential, commercial, and state-owned washing machines in California will be required to have a built-in microfibre filtering system (mesh size no higher than 100  $\mu\text{m}$ ).<sup>10</sup> The National Plastics Plan of the Australian government mandated microfiber filters in commercial and home washers by July 2030. Finally, by 2025, all new washing machines in France will be required to include a filter to catch plastic microfibres from garments.<sup>11–13</sup> In December 2019, the European Commission announced the European Green Deal (EGD) to make Europe the first climate-neutral continent by 2050.<sup>11,12</sup> In 2015 all United Nations Member States agreed to the 2030 Agenda for Sustainable Development, which is directed at achieving peace and prosperity for people and the planet. The agenda presented seventeen Sustainable Development Goals (SDGs), connecting the mission to eradicate poverty and other deprivations with targeted actions and initiatives promoting health and education, decreasing inequality, stimulating economic development, addressing climate change and preserving our seas and forests.<sup>14</sup> As legislative efforts are underway and debates are sparked on how to manage and collect this emerging micro/nano waste, it is also necessary to consider how it will be ensured that the collected plastics are not released back to the environment (through landfills for example) or contribute to climate change through their uncontrolled combustion.<sup>13</sup>

Herein, we provide proof of concept for the catalytic pyrolysis upcycling of micro/nano plastic waste into energy carriers (such as  $\text{H}_2$ ) and carbon nanotubes (as well as other nanostructured carbon products). We show that an Fe–Ni catalyst can convert the two most dominant fabrics used globally, cotton (natural fiber) and polyester (synthetic/polymer fiber)<sup>15</sup> to hydrogen and solid carbon nanomaterials. With suitable catalysts, thermal conversion technologies can be optimised to produce turquoise hydrogen and tailor the structure of the carbon products towards need. Ni-based catalysts present high reactivity for C–O and C–H bond cleavage, making them effective for polymer cracking and reforming reactions.<sup>16</sup> One of the targets of this research work was to produce as a secondary product carbon nanomaterials, such as carbon nanotubes that have attracted much interest since their discovery due to their exceptional chemical and physical properties. Other types of carbon materials can also potentially be targeted with this technology, such as graphite, graphene, carbon fibers, and amorphous carbon.<sup>13</sup>

This approach would transform harmful waste materials into useful product, while keeping carbon in the solid phase (avoiding greenhouse gas emissions). The hydrogen produced by pyrolysis of textile micro/nano fibers may be classified as turquoise hydrogen since it is produced by thermal breakdown of plastics/biomass while producing minimal emissions.<sup>13,17</sup> In addition, hydrogen has numerous industrial applications, is considered a clean fuel, is central to future energy scenarios and can be utilised to provide some of the energy necessary in the pyrolysis *via* a low emission fuel.<sup>18</sup> The global scope of the problem and the urgent need for progress necessitate ambitious collaborative efforts among fundamental scientific research, engineering development, industries, governments, and computational studies to accelerate research and develop and optimize promising processes leading to viable circular economy solutions.<sup>18</sup>

## Results and discussion

In order to model the textile fiber waste generated from washing and drying cotton and polyester fabrics, a milling method was used resulting in the length and width distributions shown in Fig. 1A and B. The fibers produced from polyester fabrics with the 40-mesh screen were between 200  $\mu\text{m}$  (0.20 mm) and 1–2 mm in length whereas the cotton fabrics produced fibers >300  $\mu\text{m}$  (0.3 mm) and max 4–7 mm in length. In terms of width, cotton fibers are thicker ( $\sim 20$   $\mu\text{m}$ ), whereas polyester fibers have a slightly thinner width ( $\sim 18$   $\mu\text{m}$ ). Fig. 1E–J shows optical and SEM images, respectively, of the fibers where the presence of fines (particles in between 0.03 to 0.05 mm in size) can be appreciated. Microfibres are defined as threadlike residues with widths of approximately 6 to 175  $\mu\text{m}$ , diameters of approximately 28  $\mu\text{m}$  on average, and lengths of approximately 250 to 6250  $\mu\text{m}$ ,<sup>19,20</sup> depending on the source of the fiber. Therefore, the particles selected can be considered as a representative sample. Due to their small size, high surface area and relatively predictable composition (formed mainly of cotton and polyester), laundry derived micro/nano textile fibers were hypothesised to form a suitable starting material for devising a thermochemical catalytic upcycling procedure aimed at making highly valuable carbon nanomaterials. Moreover, the higher surface area compared to other plastic wastes was expected to increase reactivity, facilitate better heat and mass transfer as well as have favourable interaction with catalyst.<sup>18</sup>

Polyester and cotton microfibers were catalytically pyrolysed using a Ni–Fe/ $\gamma$ - $\text{Al}_2\text{O}_3$  catalyst (details in ESI<sup>†</sup>) over a broad temperature range and showed distinct gas evolution features (Fig. 2). Both cotton and polyester released hydrocarbons as well as hydrogen during pyrolysis (Fig. 2).  $\text{H}_2$  production was at its peak at 500  $^\circ\text{C}$  for both samples but displayed a different onset temperature for cotton and PET (Fig. 2A1 and B1).  $\text{H}_2$  production occurred after the observation of other gas products of pyrolysis, which is indicative of secondary hydrocarbon cracking reactions.<sup>21</sup> Furthermore, the hydrogen production peaks were quantified (details in ESI<sup>†</sup>), which facilitated identification of temperature ranges maximising hydrogen production (Tables 3S and 4S<sup>†</sup>). Notably, the results consistently indicate that the highest production peak for both feedstocks



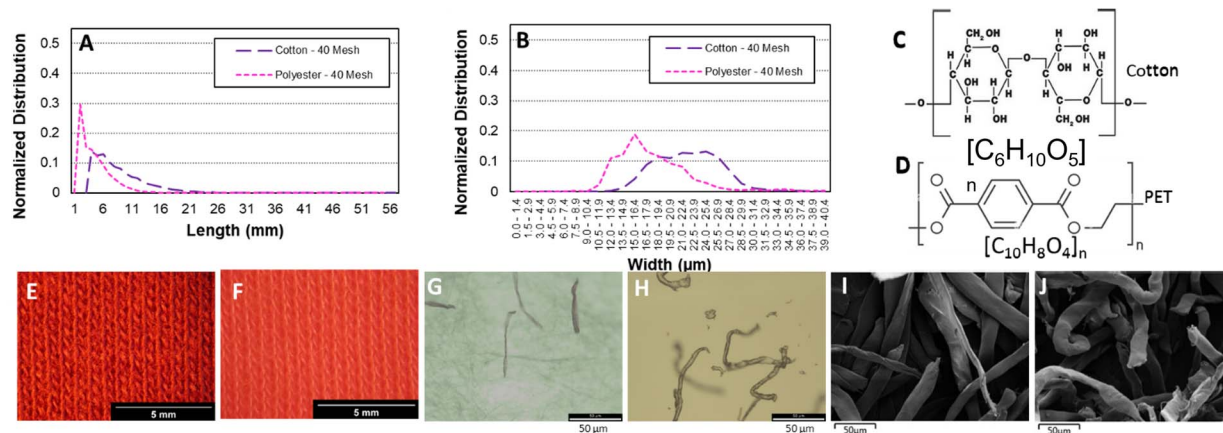


**Fig. 1** (A) Fiber length distribution of microfibers. The average fiber length 1–2 mm for PET and 4–7 mm for cotton (B) fiber width distribution of microfibers. The average fiber width is around 18  $\mu\text{m}$  for PET and 20  $\mu\text{m}$  for cotton (C) chemical formula and structure of cotton and (D) chemical formula and structure of PET. Comparing (C) and (D) cotton have more hydrogen that can be realised upon (E) and (F) optical microscope images of textiles (E) cotton and (F) PET. (G) and (H) Optical microscope pictures of fines of microfibers (G) cotton and (H) PET. (I) and (J) TEM images of microfibers (I) cotton and (J) PET showing cut/ripped ends.

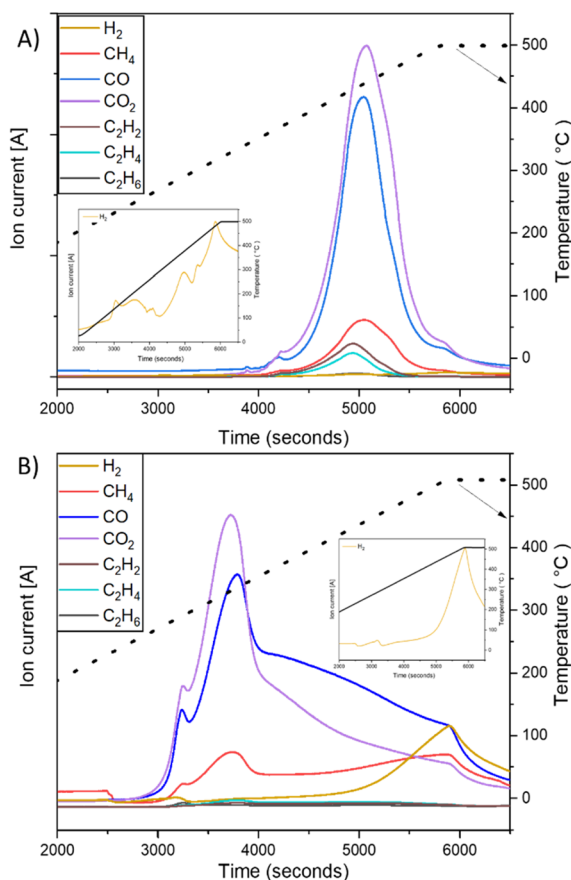


**Fig. 2** Gas evolution profile for catalytic pyrolysis experiment (with zoom of  $\text{H}_2$  evolution). (A) PET and (B) cotton.

was observed at a temperature of 500  $^{\circ}\text{C}$ . This finding emphasizes the significance of this specific temperature as the optimal condition for maximizing hydrogen production across different feedstocks. Significant insights can be gleaned from the

observed  $\text{CO}$  and  $\text{CO}_2$  production peaks depicted in Fig. 2. The data clearly indicate that the current process is not yet optimized. Consequently, the subsequent phase of this research will entail conducting a comprehensive parametric study of the process and to optimize the catalyst composition, thereby reducing the emissions of  $\text{CO}$  and  $\text{CO}_2$  while simultaneously enhancing the overall hydrogen production. By fine-tuning the catalyst composition, it is anticipated that the undesired emissions will be minimized, leading to a more efficient and environmentally friendly hydrogen production process. In an ideal application only  $\text{H}_2$  would be produced in the gas phase and emission of polluting and greenhouse gases would be avoided by adjusting the process temperature, temperature ramp rate, number of heating zones used in pyrolysis as well as catalyst structure and composition to promote secondary cracking reactions. Fig. 2 is important for illustrating catalytic pyrolysis of a well defined solid feedstock representative of laundry derived waste and forms a first step in catalyst and process optimisation. As the monomer of cotton ( $\text{C}_{10}\text{H}_{20}\text{O}_{10}$ ) contains a larger quantity of hydrogen than the monomer of PET ( $\text{C}_{10}\text{H}_8\text{O}_4$ ), the observation of a larger hydrogen production peak when cotton is used as a feedstock is consistent with the higher H/C ratio in the chemical formulae of starting feed (Fig. 2C and D).<sup>22</sup> While cotton is mainly composed of cellulose, PET is derived from terephthalic acid (TPA) and ethylene glycol (EG), and the high concentration of aromatic monomers on the backbone reduces chain mobility.<sup>15</sup>

Fig. 3A and C presents TGA and DSC during temperature programmed oxidation (TPO) of the solid products of pyrolysis (mixed with catalyst), to determine the thermal stability and chemical structure of the carbon produced. By looking at the mass loss peaks (TGA) and exothermic/endothermic features (DSC), it is possible to perform carbon nanomaterial identification on the sample. This is a common method to characterise the purity of carbon nanomaterials, *e.g.*, carbon nanotubes.<sup>16</sup> From Fig. 3A and C, three distinct mass loss regions are



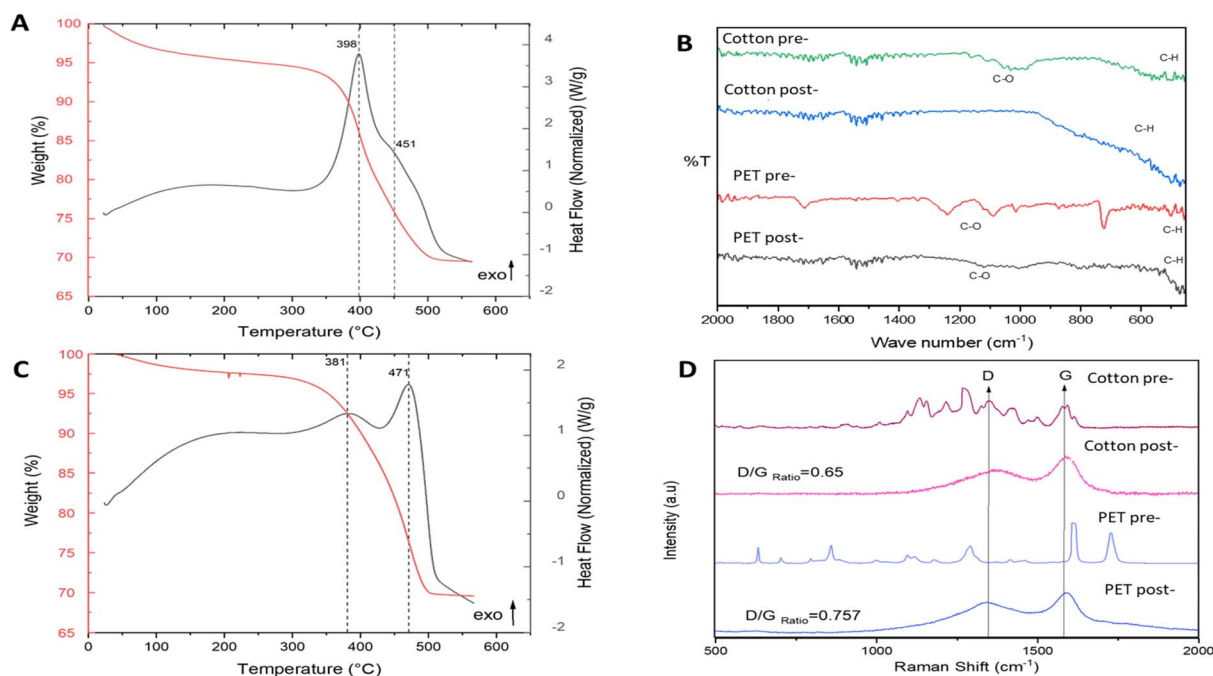


**Fig. 3** TGA and DSC curves of combustion of post-reaction samples in air atmosphere ( $5\text{ }^{\circ}\text{C min}^{-1}$ ) (A) PET and (C) cotton. Two oxidation peaks are shown in both curves, indicating the production of two different types of carbon (B) FT-IR patterns. The disappearance of C–O and C–H shows a certain degree of carbonization (D) Raman spectra of pre/post reaction cotton and PET samples (532 nm laser was used to conduct post-reaction measurements). D/G ratio indicates higher degree of graphitization when the value approaches 1.

observed: (1) under  $100\text{ }^{\circ}\text{C}$ , moisture present in the sample; (2) between  $350$  and  $450\text{ }^{\circ}\text{C}$ , combustion of amorphous carbon;<sup>16,23</sup> and (3) from  $450$  until  $700\text{ }^{\circ}\text{C}$ , associated with filamentous carbon.<sup>16,23</sup> Comparing TGA and DSC curves of the post-reaction samples with the TGA and DSC curves of the fresh samples (Fig. 2S†) a catalytic transformation is confirmed along with the presence of multiple types of carbon on the post-reaction samples. Furthermore, the solid carbon product yield was calculated (further information in ESI†) as 43% for cotton and 28% for PET. Table 1 displays the analysis of the post pyrolysis carbon products, based on their oxidation temperatures. It can be observed that cotton pyrolysis results in a major percentage of filamentous carbon.

Raman and FT-IR measurements validate the TGA-DSC results. FT-IR (Fig. 3B) shows that thermal treatment produced clear destruction of the C=O and C–H chemical functionalities of both cotton and PET, indicative of a high degree of carbonisation.

Raman spectroscopy (Fig. 3D) also shows notable differences in cotton and PET after catalytic pyrolysis. The appearance of two characteristic peaks at around  $1350$  and  $1580$  in the post-

pyrolysis samples are indicative of  $\text{sp}^2$  bonded carbon.<sup>24</sup> The Raman spectra of disordered graphite exhibits two modes, the G peak at  $1580\text{--}1600\text{ cm}^{-1}$  and the D peak at  $1350\text{ cm}^{-1}$ , which are often attributed to phonons with  $\text{E}_{2g}$  and  $\text{A}_{1g}$  symmetry, respectively.<sup>25</sup> The existence of the D peak band can indicate the presence of aromatic compounds with a ring size greater than six fused rings.<sup>26</sup> G band is commonly referred to as the “graphite band” because it involves the in-plane bond-stretching motion of pairs of C  $\text{sp}^2$  atoms ( $\text{E}_{2g}$ ), whereas D band is commonly referred to as the “defect band” because it provides information about the morphological disorder and defects that are characteristic of disordered graphite ( $\text{A}_{1g}$ ).<sup>24</sup> As it can be appreciated in Fig. 3D, the shape and position of these bands differ slightly across the different cotton and PET post-reaction samples indicating structural differences between the carbonaceous structures produced by catalytic pyrolysis of the fresh samples. The D band is shifted towards higher Raman shift values in the cotton post-reaction sample, while the G band is quite stable in the same value for both post-reaction samples (cotton and PET). The D band is a double-resonant process in Raman. When the number of defects rise, the D

**Table 1** Distribution of carbon products of cotton and PET pyrolysis, determined *via* TGA-DSC

|        | Amorphous C oxidation temperature ( $^{\circ}\text{C}$ ) | wt% of total carbon product | Filamentous carbon oxidation temperature ( $^{\circ}\text{C}$ ) | wt% of total carbon product |
|--------|--|-----------------------------|---|-----------------------------|
| Cotton | 380  | 41                          | 470   | 51                          |
| PET    | 400  | 63                          | 450   | 37                          |



band usually moves to higher frequencies.<sup>24</sup> The ratio of the intensities of these bands (D/G) is a crucial parameter for distinguishing the defect concentration of carbon generated during thermal decomposition caused by catalytic pyrolysis processes.<sup>27</sup> The conversion of nano-crystalline graphite to amorphous carbon increases the D/G ratio.<sup>27</sup> Graphitic materials have a prominent G peak due to  $sp^2$  bound carbon atoms' tangential vibration modes.<sup>28–30</sup> The D/G ratio varies widely depending on the type of CNT material. The D/G ratio of many multiwall CNT-based materials is between 0.27 and 0.90.<sup>31,32</sup> Single-walled and double-walled CNTs (SWCNTs and DWCNTs, respectively) have higher D/G ratio, for 532 nm laser excitation, from 0.09 as-is to 0.01 purified, and from 0.12 as-is to 0.04 purified (for 785 nm laser excitation). These D/G ratios qualitatively indicate purity and crystalline structure.<sup>33–35</sup> The D/G ratio value obtained for the cotton and PET post-reaction samples were 0.65 and 0.75 respectively. This shows that carbon produced by the utilization of cotton as feedstock is more graphitised.<sup>36</sup> SEM-EDX (Fig. 4) was used to characterise the growth/deposition of carbon nanostructures on the catalyst and showed that carbon was co-located with Ni and Fe, indicating a gas phase cracking reaction on the catalyst rather than a solid-to-solid transformation.<sup>21</sup> Further investigation *via* TEM-

EDX revealed that catalyst sintering has occurred during reaction and identified stabilization of nano-alloys of Ni and Fe as a promising path forward to produce size-controlled carbon nanotubes.

Our pyrolysis proof of concept experiments, together with characterisation show that it is possible to produce hydrogen *via* chemical processes from both cotton and polyester microfibre waste, modelling the majority feedstock of waste that can be collected from laundering, drying, and vacuuming with the use of filters. We show that filamentous carbon and hydrogen can be produced from both cotton and polyester, indicating a process could be developed for catalytic upcycling of mixed microfibre waste. Improvements in catalyst formulation and especially stability are key, as we have observed some agglomeration of NiFe nanoparticles (Fig. 1S†), the proposed active phase for the growth of filamentous carbon. Process improvements can include a dual reactor configuration where microfibre waste can be heated to a lower temperature while the catalytic pyrolysis would be performed above 500 °C, which can achieve greater selectivity over products due to the separation of the gasification and cracking steps. The production of hydrogen (which can be called turquoise hydrogen due to the carbon remaining in the solid phase) through this process is significant for offering a low emission source of heat to drive the thermochemical upcycling process. Based on the chemical formula of polyester, the heat of pyrolysis<sup>22</sup> and the lower heating value of hydrogen gas, it is estimated that up to 19% of the energy requirement for pyrolysis of polyester can be provided by the  $H_2$  released from reaction (details in ESI†). While the process will require external energy input, it can still serve as a low emission alternative for the synthesis of carbon nanotubes which have a vastly growing demand, and the state-of-the-art processes for their production all rely on fossil fuel derivatives as reactant. Moreover, upon shifting the mix of textiles used in society to depend less on fossil derivatives and more on biobased alternatives, the resulting changes in fibrous feedstock can further lower the carbon footprint of fibers derived carbon nanotubes.

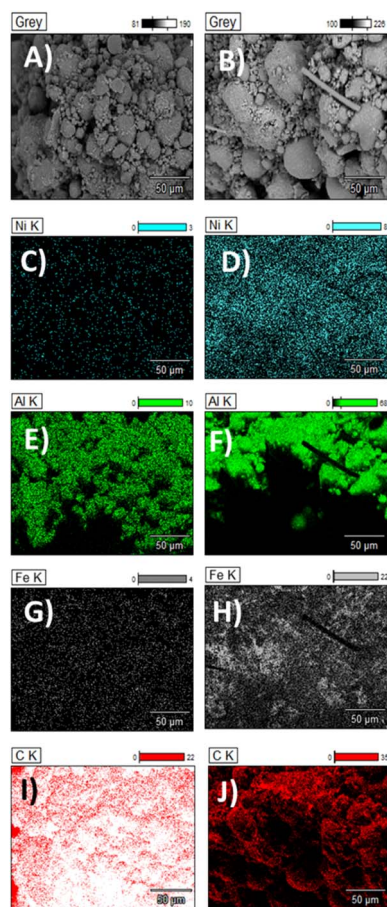


Fig. 4 SEM-EDX images. (A, C, E, G, I) Cotton post-reaction and (B, D, F, H, J) PET post-reaction. Carbon growth over the catalyst particle can be appreciated.

## Conclusions

Herein, we have demonstrated a controlled proof of concept for the catalytic pyrolysis behaviour of the two most common microfibre wastes released from laundering fabrics. A process temperature of 500 °C has been shown to be necessary for  $H_2$  production from both cotton and polyester. We showed *via* FT-IR, Raman, TGA-DSC, SEM-EDX, TEM-EDX that both cotton and PET yielded filamentous carbons, with cotton microfibers generating more graphitised carbonaceous material. This is a novel approach to upcycle the most difficult type of waste (microfibers) among 92 million tonnes of waste generated annually by the fashion industry, most of which is incinerated, landfilled, or exported to developing countries.<sup>37</sup> Based on this foundational proof of concept, the design of stable catalysts with control over carbon product selectivity can enable the integration of microfibre waste into a circular economy, reducing the impact of fast fashion on the climate as well as land and water ecosystems.



## Author contributions

S. Parrilla-Lahoz: writing-original draft, conceptualization, visualization, and investigation. Marielis C. Zambrano: investigation, writing-review, and editing. Vlad Stolojan: writing review, investigation, and editing. Rachida Bance-Soualhi: writing review, investigation, and editing. Joel J. Pawlak: writing-review, funding acquisition, supervision, writing-review, and editing. Richard A. Venditti: writing-review, funding acquisition, supervision, writing-review, and editing. Tomas. R. Reina: writing-review, funding acquisition, conceptualization, project administration and supervision. Melis S. Duyar: writing-review, funding acquisition, supervision, conceptualization, visualization, project administration and writing-review and editing.

## Conflicts of interest

The authors declare that they have no known competing financial interests or personal relationships that could have appeared to influence the work reported in this paper.

## Acknowledgements

Financial support for this work was provided primarily by the University Global Partnership Network (UGPN) Research Collaboration Fund (RCF) and the School of Chemistry and Chemical Engineering at University of Surrey. SPL acknowledges the University of Surrey Breaking Barriers Fellowship for funding her doctoral studies.

## References

- 1 T. R. Walker and L. Fequet, Current trends of unsustainable plastic production and micro(nano)plastic pollution, *TrAC, Trends Anal. Chem.*, 2023, **160**, 116984, DOI: [10.1016/j.trac.2023.116984](https://doi.org/10.1016/j.trac.2023.116984).
- 2 PlasticsEurope (PEMRG), *Annual production of plastics worldwide from 1950 to 2021 (in million metric tons) [Graph]*, In Statista, December 2, 2022, retrieved April 20, 2023, from <https://www.statista.com/statistics/282732/global-production-of-plastics-since-1950/>.
- 3 X. Guo and J. Wang, The chemical behaviors of microplastics in marine environment: a review, *Mar. Pollut. Bull.*, 2019, **142**, 1–14, DOI: [10.1016/j.marpolbul.2019.03.019](https://doi.org/10.1016/j.marpolbul.2019.03.019).
- 4 J. Liu, J. Liang, J. Ding, G. Zhang, X. Zeng, Q. Yang, B. Zhu and W. Gao, Microfiber pollution: an ongoing major environmental issue related to the sustainable development of textile and clothing industry, *Environ. Dev. Sustain.*, 2021, **23**, 11240–11256, DOI: [10.1007/s10668-020-01173-3](https://doi.org/10.1007/s10668-020-01173-3).
- 5 S. Haslinger, Y. Wang, M. Rissanen, M. B. Lossa, M. Tanttu, E. Ilen, M. Määttä, A. Harlin, M. Hummel and H. Sixta, Recycling of vat and reactive dyed textile waste to new colored man-made cellulose fibers, *Green Chem.*, 2019, **21**, 5598–5610, DOI: [10.1039/c9gc02776a](https://doi.org/10.1039/c9gc02776a).
- 6 S. Asaadi, M. Hummel, S. Hellsten, T. Härkäsalmi, Y. Ma, A. Michud and H. Sixta, Renewable High-Performance Fibers from the Chemical Recycling of Cotton Waste Utilizing an Ionic Liquid, *ChemSusChem*, 2016, **9**, 3250–3258, DOI: [10.1002/cssc.201600680](https://doi.org/10.1002/cssc.201600680).
- 7 S. J. Royer, K. Wiggin, M. Kogler and D. D. Deheyn, Degradation of synthetic and wood-based cellulose fabrics in the marine environment: comparative assessment of field, aquarium, and bioreactor experiments, *Sci. Total Environ.*, 2021, 791, DOI: [10.1016/j.scitotenv.2021.148060](https://doi.org/10.1016/j.scitotenv.2021.148060).
- 8 M. C. Zambrano, J. J. Pawlak, J. Daystar, M. Ankeny, C. C. Goller and R. A. Venditti, Aerobic biodegradation in freshwater and marine environments of textile microfibers generated in clothes laundering: effects of cellulose and polyester-based microfibers on the microbiome, *Mar. Pollut. Bull.*, 2020, **151**, 110826, DOI: [10.1016/j.marpolbul.2019.110826](https://doi.org/10.1016/j.marpolbul.2019.110826).
- 9 M. C. Zambrano, J. J. Pawlak, J. Daystar, M. Ankeny, J. J. Cheng and R. A. Venditti, Microfibers generated from the laundering of cotton, rayon and polyester based fabrics and their aquatic biodegradation, *Mar. Pollut. Bull.*, 2019, **142**, 394–407, DOI: [10.1016/j.marpolbul.2019.02.062](https://doi.org/10.1016/j.marpolbul.2019.02.062).
- 10 *California-2023-AB1628-Amended*, <https://legiscan.com/CA/text/AB1628/id/2756328>, accessed May 10, 2023.
- 11 European Green Deal, 2020, [https://commission.europa.eu/strategy-and-policy/priorities-2019-2024/european-green-deal\\_es](https://commission.europa.eu/strategy-and-policy/priorities-2019-2024/european-green-deal_es), accessed May 10, 2023.
- 12 *A European strategy for plastics in a circular economy*, 2015, <https://ec.europa.eu/environment/pdf/circular-economy/plastics-strategy.pdf>, accessed May 10, 2023.
- 13 S. Parrilla-Lahoz, S. Mahebadegan, M. Kauta, M. C. Zambrano, J. J. Pawlak, R. A. Venditti, T. R. Reina and M. S. Duyar, Materials challenges and opportunities to address growing micro/nanoplastics pollution: a review of thermochemical upcycling, *Mater. Today Sustain.*, 2022, **20**, 100200, DOI: [10.1016/j.mtsust.2022.100200](https://doi.org/10.1016/j.mtsust.2022.100200).
- 14 U. Nations, *The 2030 Agenda and the Sustainable Development Goals an Opportunity for Latin America and the Caribbean Goals, Targets and Global Indicators*, 2030. <http://www.issuu.com/publicacionescepal/stacks>.
- 15 K. Subramanian, M. K. Sarkar, H. Wang, Z. H. Qin, S. S. Chopra, M. Jin, V. Kumar, C. Chen, C. W. Tsang and C. S. K. Lin, An overview of cotton and polyester, and their blended waste textile valorisation to value-added products: a circular economy approach—research trends, opportunities and challenges, *Crit. Rev. Environ. Sci. Technol.*, 2022, **52**, 3921–3942, DOI: [10.1080/10643389.2021.1966254](https://doi.org/10.1080/10643389.2021.1966254).
- 16 D. Yao, C. Wu, H. Yang, Y. Zhang, M. A. Nahil, Y. Chen, P. T. Williams and H. Chen, Co-production of hydrogen and carbon nanotubes from catalytic pyrolysis of waste plastics on Ni-Fe bimetallic catalyst, *Energy Convers. Manag.*, 2017, **148**, 692–700, DOI: [10.1016/j.enconman.2017.06.012](https://doi.org/10.1016/j.enconman.2017.06.012).
- 17 A. M. Amin, E. Croiset and W. Epling, Review of methane catalytic cracking for hydrogen production, *Int. J. Hydrogen*



- Energy*, 2011, **36**, 2904–2935, DOI: [10.1016/j.ijhydene.2010.11.035](https://doi.org/10.1016/j.ijhydene.2010.11.035).
- 18 The Pew Charitable Trusts, *Breaking the Plastic Wave: A Comprehensive Assessment of Pathways towards Stopping Ocean Plastic Pollution*, 2020, vol. 56.
- 19 M. Yamin, P. I. Hynd, R. W. Ponzoni, J. A. Hill, W. S. Pitchford, K. A. Hansford, M. Yamin, P. I. Hyndl, R. K. Ponzoniz, J. A. Hill, K. S. Pitchford and A. A. Hansford, *Is Fibre Diameter Variation along the Staple a Good Indirect Selection Criterion for Staple Strength?*, 1999.
- 20 S. A. Carr, Sources and dispersive modes of micro-fibers in the environment, *Integr. Environ. Assess. Manag.*, 2017, **13**, 466–469, DOI: [10.1002/ieam.1916](https://doi.org/10.1002/ieam.1916).
- 21 P. T. Williams, Hydrogen and Carbon Nanotubes from Pyrolysis-Catalysis of Waste Plastics: A Review, *Waste Biomass Valorization*, 2021, **12**, 1–28, DOI: [10.1007/s12649-020-01054-w](https://doi.org/10.1007/s12649-020-01054-w).
- 22 H. Peng, P. Li and Q. Yang, Investigation on the reaction kinetics, thermodynamics and synergistic effects in co-pyrolysis of polyester and viscose fibers, *React. Kinet. Mech. Catal.*, 2022, **135**, 769–793, DOI: [10.1007/s11144-022-02167-0](https://doi.org/10.1007/s11144-022-02167-0).
- 23 R. X. Yang, S. L. Wu, K. H. Chuang and M. Y. Wey, Co-production of carbon nanotubes and hydrogen from waste plastic gasification in a two-stage fluidized catalytic bed, *Renew. Energy*, 2020, **159**, 10–22, DOI: [10.1016/j.renene.2020.05.141](https://doi.org/10.1016/j.renene.2020.05.141).
- 24 R. Volpe, J. M. Bermudez Menendez, T. Ramirez Reina, M. Volpe, A. Messineo, M. Millan and M. M. Titirici, Free radicals formation on thermally decomposed biomass, *Fuel*, 2019, **255**, 115802, DOI: [10.1016/j.fuel.2019.115802](https://doi.org/10.1016/j.fuel.2019.115802).
- 25 M. S. Dresselhaus, G. Dresselhaus, A. Jorio, A. G. Souza Filho and R. Saito, Raman spectroscopy on isolated single wall carbon nanotubes, *Carbon*, 2002, **40**, 2043–2061, DOI: [10.1016/S0008-6223\(02\)00066-0](https://doi.org/10.1016/S0008-6223(02)00066-0).
- 26 M. Asadullah, S. Zhang, Z. Min, P. Yimsiri and C. Z. Li, Effects of biomass char structure on its gasification reactivity, *Bioresour. Technol.*, 2010, **101**, 7935–7943, DOI: [10.1016/j.biortech.2010.05.048](https://doi.org/10.1016/j.biortech.2010.05.048).
- 27 M. S. Dresselhaus, G. Dresselhaus, A. Jorio, A. G. S. Filho and R. Saito, *Raman Spectroscopy on Isolated Single Wall Carbon Nanotubes*, 2002.
- 28 R. Saito, M. Hofmann, G. Dresselhaus, A. Jorio and M. S. Dresselhaus, Raman spectroscopy of graphene and carbon nanotubes, *Adv. Phys.*, 2011, **60**, 413–550, DOI: [10.1080/00018732.2011.582251](https://doi.org/10.1080/00018732.2011.582251).
- 29 M. S. Dresselhaus, A. Jorio, A. G. Souza Filho and R. Saito, Defect characterization in graphene and carbon nanotubes using Raman spectroscopy, *Phil. Trans. Math. Phys. Eng. Sci.*, 2010, **368**, 5355–5377, DOI: [10.1098/rsta.2010.0213](https://doi.org/10.1098/rsta.2010.0213).
- 30 A. C. Ferrari and D. M. Basko, Raman spectroscopy as a versatile tool for studying the properties of graphene, *Nat. Nanotechnol.*, 2013, **8**, 235–246, DOI: [10.1038/nnano.2013.46](https://doi.org/10.1038/nnano.2013.46).
- 31 R. A. DiLeo, B. J. Landi and R. P. Raffaele, Purity assessment of multiwalled carbon nanotubes by Raman spectroscopy, *J. Appl. Phys.*, 2007, **101**(6), 064307, DOI: [10.1063/1.2712152](https://doi.org/10.1063/1.2712152).
- 32 J. H. Pöhls, M. B. Johnson, M. A. White, R. Malik, B. Ruff, C. Jayasinghe, M. J. Schulz and V. Shanov, Physical properties of carbon nanotube sheets drawn from nanotube arrays, *Carbon*, 2012, **50**, 4175–4183, DOI: [10.1016/j.carbon.2012.04.067](https://doi.org/10.1016/j.carbon.2012.04.067).
- 33 N. Behabtu, C. C. Young, D. E. Tsentelovich, O. Kleinerman, X. Wang, A. W. K. Ma, E. Amram Bengio, R. F. ter Waarbeek, J. J. de Jong, R. E. Hoogerwerf, S. B. Fairchild, J. B. Ferguson, B. Maruyama, J. Kono, Y. Talmon, Y. Cohen, M. J. Otto and M. Pasquali, *Strong, Light, Multifunctional Fibers of Carbon Nanotubes with Ultrahigh Conductivity*, 2013, <http://www.sciencemag.org>.
- 34 R. Rao, J. Reppert, R. Podila, X. Zhang, A. M. Rao, S. Talapatra and B. Maruyama, Double resonance Raman study of disorder in CVD-grown single-walled carbon nanotubes, *Carbon*, 2011, **49**, 1318–1325, DOI: [10.1016/j.carbon.2010.11.052](https://doi.org/10.1016/j.carbon.2010.11.052).
- 35 Y. Zhao, J. Wei and R. Vajtai, Iodine doped carbon nanotube cables exceeding specific electrical conductivity of metals, *Sci. Rep.*, 2011, **1**, 83.
- 36 J. S. Bulmer, T. S. Gspann, J. S. Barnard and J. A. Elliott, Chirality-independent characteristic crystal length in carbon nanotube textiles measured by Raman spectroscopy, *Carbon*, 2017, **115**, 672–680, DOI: [10.1016/j.carbon.2017.01.044](https://doi.org/10.1016/j.carbon.2017.01.044).
- 37 K. Niinimäki, G. Peters, H. Dahlbo, P. Perry, T. Rissanen and A. Gwilt, The environmental price of fast fashion, *Nat. Rev. Earth Environ.*, 2020, **1**, 189–200, DOI: [10.1038/s43017-020-0039-9](https://doi.org/10.1038/s43017-020-0039-9).

